

Kinetically-Enhanced Anomaly Mediation

Abhishek Kumar, David E. Morrissey, and Andrew Spray

TRIUMF, 4004 Wesbrook Mall, Vancouver, BC V6T 2A3, Canada.

email: abhishek@triumf.ca, dmorri@triumf.ca, aps37@triumf.ca

February 2, 2022

Abstract

We investigate a modification of anomaly-mediated supersymmetry breaking (AMSB) with an exotic $U(1)_x$ gauge sector that can solve the tachyonic slepton problem of minimal AMSB scenarios. The new $U(1)_x$ multiplet is assumed to couple directly to the source of supersymmetry breaking, but only indirectly to the minimal supersymmetric Standard Model (MSSM) through kinetic mixing with hypercharge. If the MSSM sector is also sequestered from the source of supersymmetry breaking, the contributions to the MSSM soft terms come from both AMSB and the $U(1)_x$ kinetic coupling. We find that this arrangement can give rise to a flavour-universal, phenomenologically viable, and distinctive spectrum of MSSM superpartners. We also investigate the prospects for discovery and the most likely signatures of this scenario at the Large Hadron Collider (LHC).

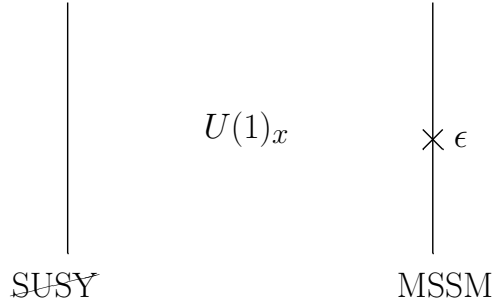


Figure 1: Schematic diagram of the visible, $U(1)_x$, and supersymmetry-breaking sectors.

1 Introduction

Supersymmetry is one of the leading candidates for new physics beyond the Standard Model (SM). To be consistent with existing experimental searches, the SM superpartners must have supersymmetry-breaking masses near the electroweak scale. The underlying nature of supersymmetry breaking plays a central role in determining the mass spectrum and the interactions of these new superpartner states, and therefore also the predictions of the theory at particle colliders. The current LHC era holds the promise of discovering superparticles and might also shed light on the nature of supersymmetry breaking. Thus it is all the more important to focus on supersymmetry breaking and to understand its origin.

A variety of mechanisms have been proposed to explain the breaking of supersymmetry and its mediation to the SM superpartners. The leading candidates include gravity mediation, gauge mediation, and anomaly mediation. Anomaly-mediated supersymmetry breaking (AMSB) is particularly compelling because it avoids introducing too much flavour mixing to the superpartner interactions and it relies only on fields present in the minimal supergravity multiplet [1, 2]. Unfortunately, AMSB in its simplest form also predicts negative soft squared masses for the sleptons that would induce an unacceptable spontaneous breakdown of electromagnetism. To remedy the situation, many solutions have been proposed to generate a viable slepton spectrum such as non-decoupling thresholds that produce additional gauge mediation [3, 4, 5, 6, 7, 8], new D -term contributions to the scalar masses [9, 10], unsequestered vector multiplets [11, 12, 13, 14], new couplings involving the lepton multiplets that persist to low energies [15, 16], and moderate additional gravity-mediated contributions [17, 18, 19].

In the present work we investigate a new mechanism for fixing the negative slepton squared mass problem of AMSB that relies on supersymmetric kinetic mixing between an unsequestered $U(1)_x$ gauge symmetry and hypercharge. It is similar to but distinct from the approaches used in Refs. [13, 14]. A schematic diagram of our proposal is shown in Fig. 1. As in standard AMSB, the minimal supersymmetric extension of the Standard Model (MSSM) is *sequestered* from the source of supersymmetry breaking. This can potentially arise from a localization of the corresponding fields in different regions in an extra dimension [1, 20, 21] or through the effects of conformal running [22, 23]. Despite the sequestering, supersym-

metry breaking is still communicated to the MSSM through universal interactions with the supergravity multiplet. We augment this minimal picture with an exotic $U(1)_x$ gauge sector that is not sequestered from supersymmetry breaking and that therefore receives large direct contributions to its soft spectrum from standard gravity mediation. The additional supersymmetry breaking present in the $U(1)_x$ sector is then communicated to the MSSM through gauge kinetic mixing with hypercharge, modifying the mass spectrum of MSSM superpartners and potentially solving the problem of negative slepton squared masses.

The outline of this paper is as follows. In Section 2 we describe in more detail the underlying extension of the MSSM and its effect on the mass spectrum of the SM superpartners. Next, in Section 3 we show that these modifications can lead to a phenomenologically viable spectrum. In Section 4 we investigate the collider signatures of this scenario, while Section 5 is reserved for our conclusions. Some accompanying technical details can be found in Appendices A and B.

2 Couplings and Soft Terms

Our theory consists of the MSSM together with an exotic supersymmetric x sector. The x sector contains a $U(1)_x$ gauge multiplet, and a pair of chiral multiplets H and H' with equal and opposite $U(1)_x$ charges $\pm x_H$ and superpotential

$$W_x = \mu' H H' . \quad (1)$$

The x and visible sectors couple only via supersymmetric gauge kinetic mixing,

$$\mathcal{L} \supset \int d^2\theta \left(\frac{\epsilon}{2} B^\alpha X_\alpha + \frac{1}{4} X^\alpha X_\alpha + \frac{1}{4} B^\alpha B_\alpha \right) + \text{h.c.} \quad (2)$$

where B_α and X_α are the gauge field strengths of $U(1)_Y$ and $U(1)_x$ respectively. This mixing interaction can be generated by integrating out massive chiral multiplets charged under both gauge groups [24] giving rise to natural values of $\epsilon \sim 10^{-4}$ – 10^{-2} . We treat the kinetic mixing coupling as a free parameter with the only condition that $\epsilon \ll 1$.

2.1 Supersymmetry Breaking and Sequestering

We assume that the MSSM sector is sequestered from the source of supersymmetry breaking, but that the $U(1)_x$ sector is not. This can be realized by localizing the MSSM away from supersymmetry breaking in a warped extra-dimensional setup [1, 20, 21], or through the effects of conformal running [22, 23]. We assume further that the source of gauge kinetic mixing is also sequestered. A schematic picture of the sequestering is given in Fig. 1.

In this framework the dominant source of supersymmetry breaking in the x sector comes from direct gravity mediation. Typical soft terms in the x sector are therefore

$$M_x \sim \sqrt{|m_H^2|} \sim \sqrt{|m_{H'}^2|} \sim \sqrt{b'} \sim m_{3/2}, \quad (3)$$

where M_x is the $U(1)_x$ gaugino soft mass, $m_{H,H'}^2$ are the soft squared masses of H and H' , b' is the bilinear holomorphic soft term mixing H and H' , and $m_{3/2}$ is the gravitino mass. These soft masses are not calculable without an ultraviolet completion incorporating supergravity and we treat them as free parameters on the order of $m_{3/2}$.¹ The dimensionful supersymmetric coupling μ' appearing in Eq. (1) can also be generated with $\mu' \sim m_{3/2}$ via the Giudice-Masiero mechanism [25], as can the corresponding soft coupling b' . Negative values of m_H^2 or $m_{H'}^2$ can induce the spontaneous breakdown of $U(1)_x$ with natural values of $\langle H \rangle \sim \langle H' \rangle \sim m_{3/2}/g_x$, leading to a massive Z_x vector of mass $m_x \sim m_{3/2}$.

Soft supersymmetry breaking terms in the MSSM sector will be generated by anomaly mediation together with direct mediation from the x sector via gauge kinetic mixing. As such, they will be suppressed relative to the soft breaking parameters in the x sector due to sequestering and the small value of the kinetic mixing coupling ϵ . We present a prescription to compute the MSSM soft terms below, and we give a derivation of this prescription in Appendix A.

2.2 MSSM Soft Masses

Supersymmetry breaking couplings in the MSSM receive contributions from anomaly mediation and from gauge kinetic mixing with the unsequestered x sector. In computing these soft terms, we take Λ to be the characteristic mass scale of the sequestering dynamics, such as the compactification scale of an extra dimension or the exit scale from a period of conformal running. With an eye on grand unification, we choose $\Lambda = 2 \times 10^{16}$ GeV, but other values could be considered. For simplicity, we also identify Λ with the (sequestered) dynamics giving rise to gauge kinetic mixing, such as a vector-like pair of chiral multiplets charged under both $U(1)_x$ and hypercharge with a supersymmetric mass on the order of Λ .

At scale Λ , the MSSM soft masses are dominated by the usual contributions from anomaly mediation evaluated at that scale, given explicitly in Refs. [1, 20, 26]. We take this to be our high-energy boundary condition. Additional threshold corrections as well as the anomaly-mediated contribution of the gauge kinetic mixing interaction are parametrically smaller. In the course of renormalization group (RG) evolution down from Λ , the MSSM soft masses receive additional contributions from the x sector. At one-loop order the MSSM gaugino masses remain unchanged. For the scalar soft masses, we find (to quadratic order in $\epsilon \ll 1$)

$$(4\pi)^2 \frac{dm_i^2}{dt} = (4\pi)^2 \left(\frac{dm_i^2}{dt} \right)_{MSSM} - \frac{24}{5} Y_i^2 \epsilon^2 g_1^2 |M_x|^2 - 2\sqrt{\frac{3}{5}} Y_i g_1 g_x \epsilon S_x \quad (4)$$

where $t = \ln(Q/m_Z)$ is the logarithm of the renormalization scale Q , $S_x = x_H(m_H^2 - m_{H'}^2)$, and M_x is the x -sector gaugino mass. The first new contribution is analogous to gaugino mediation [27, 28] and is generated by diagrams of the form shown in the left panel of Fig. 2, while the second comes from diagrams like in the right panel of this figure. The one-loop

¹ For $M_x, \sqrt{b'} \sim m_{3/2}$ it is also necessary that the source of supersymmetry breaking involves gauge singlets.

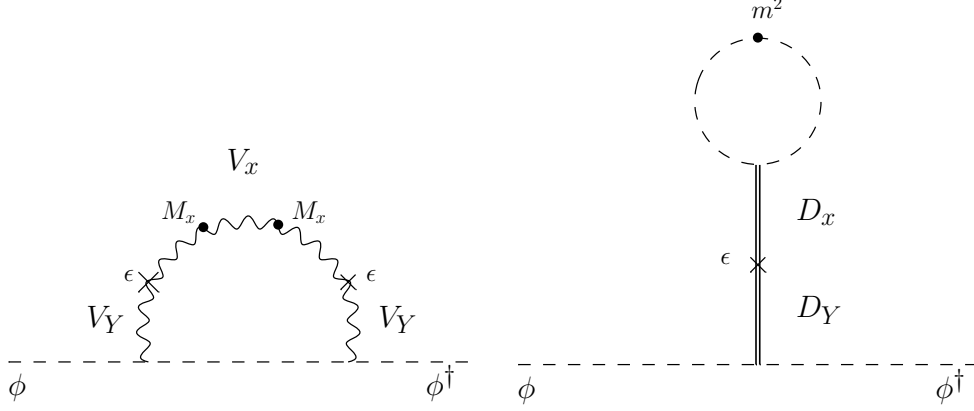


Figure 2: Contributions to the RG running of the MSSM scalar soft masses from supersymmetric gauge kinetic mixing between hypercharge and $U(1)_x$. The left panel shows the leading effect from the mixing of the gaugino components, while the right panel illustrates the contribution from the mixing of the D -terms.

running of the trilinear A terms is given by (to quadratic order in $\epsilon \ll 1$)

$$(4\pi)^2 \frac{dA_f}{dt} = (4\pi)^2 \left(\frac{dA_f}{dt} \right)_{MSSM} + \frac{12}{5} \sum_i Y_i^2 g_1^2 \epsilon^2 M_x, \quad (5)$$

where the sum in the second term runs over the hypercharges of all the fields involved in the corresponding interaction. This contribution is generated by diagrams of the form of Fig. 2, but with only a single M_x insertion. RG equations for M_x and $m_{H,H'}^2$ are given in Appendix A.

These RG equations only apply at energies larger than the x -sector masses, on the order of $m_{3/2}$. At $Q = m_{3/2}$ we integrate out the heavy x -sector multiplets. The main effect of doing so is to generate an effective Fayet-Iliopoulos (FI) term [29] for hypercharge from the vacuum expectation values (VEVs) of H and H' inducing the spontaneous breakdown of $U(1)_x$. Writing

$$\langle H \rangle = v_x \sin \alpha, \quad \langle H' \rangle = v_x \cos \alpha, \quad (6)$$

we have $m_x = \sqrt{2} g_x c_\epsilon x_H v_x$ for the $U(1)_x$ vector mass, where $c_\epsilon = 1/\sqrt{1-\epsilon^2}$. Up to an overall constant, the induced FI term can be absorbed in the MSSM soft scalar masses according to (to quadratic order in $\epsilon \ll 1$)

$$m_i^2(Q = m_{3/2}^-) = m_i^2(Q = m_{3/2}^+) + \frac{\epsilon}{2} \sqrt{\frac{3}{5}} \frac{Y_i}{x_H} \frac{g_1}{g_x} m_x^2 \cos 2\alpha. \quad (7)$$

The RG running of the MSSM soft terms from $m_{3/2}$ to near the electroweak scale is identical to the MSSM. More details about the prescription given here for computing the MSSM soft masses are given in Appendix A.

From the discussion above we see that, in addition to anomaly mediation, the MSSM soft scalar masses get contributions from the $U(1)_x$ gauginos that push them towards more positive values, as well as contributions from S_x and $U(1)_x$ breaking that are proportional to hypercharge and can have either sign. We will show below that the positive effect of the unsequestered $U(1)_x$ gaugino mass can yield a phenomenologically viable soft mass spectrum for the MSSM. In particular, this scenario can evade the tachyonic slepton problem of minimal anomaly mediation.

There are two additional important differences between this scenario and pure anomaly mediation. First, the MSSM soft masses depend implicitly on high-scale physics, and are therefore not UV insensitive. This is the result of the overall mass scale in the x sector being of the same order as the scale of supersymmetry breaking in that sector. Second, to get $M_x \sim m_{3/2}$, a necessary condition for positive MSSM soft masses, the supersymmetry breaking sector must contain gauge singlets, which is not the case for pure anomaly mediation.

A slight variation on this scenario that could lead to positive soft masses for all MSSM scalars in the absence of a supersymmetry-breaking singlet (or for small values of ϵ) would be to gauge a sequestered $(B-L)$ and to arrange for it to also have kinetic mixing with $U(1)_X$. In this case, both hypercharge and $(B-L)$ D -terms would be generated by the x sector. As shown in Refs. [9, 10], such terms can yield positive MSSM soft scalar masses while retaining the UV insensitivity property of minimal AMSB. We defer a study of this variation to a future work.

3 X -Sector Parameters and MSSM Spectra

Based on our discussion in the previous section, we can derive the low-energy MSSM spectrum once we specify the parameter values in the x sector (along with μ and $B\mu$ in the MSSM sector). While the x sector is relatively unconstrained, there are evidently many phenomenological constraints on the visible sector, such as consistent electroweak symmetry breaking, precision electroweak tests, and direct collider constraints on particle masses. In this section we perform a scan over parameter values in the x sector to search for viable MSSM spectra.

3.1 Symmetry Breaking in the X Sector

The independent parameters characterizing the x sector are ϵ , $g_x x_H$, μ' , b' , M_x , m_H^2 , and $m_{H'}^2$. Of these, the first three are supersymmetric while the remaining four arise from soft supersymmetry breaking. We demand that the $U(1)_x$ gauge symmetry be spontaneously broken. The corresponding minimization conditions for H and H' allow us to replace two of these parameters with the massive Z_x vector mass m_x and the ratio of VEVs $\tan \alpha$. We choose to solve for b' , m_H^2 , and $m_{H'}^2$ in terms of m_x , $\tan \alpha$, and $S_x/x_H = (m_H^2 - m_{H'}^2)$.

Parameter	Range
ϵ	$[0.01, 0.1]$
$g_x x_H$	$[0.7, 0.9]$
M_x	$[0.5, 5] \times m_{3/2}$

Parameter	Range
S_x/x_H	$[-5, 5] \times m_{3/2}^2$
m_x	$[0.1, 10] \times m_{3/2}$
$\tan \alpha$	$[0, 0.75] \cup [1.25, 50]$
μ'	$[0.5, 5] \times m_{3/2}$

Table 1: Input parameters in the x sector specified at the high scale Λ (left) and the lower scale $m_{3/2}$ (right), and the corresponding scan ranges considered in our analysis.

The leading part of the x -sector scalar potential is

$$V = (|\mu'|^2 + m_H^2)|H|^2 + (|\mu'|^2 + m_{H'}^2)|H'|^2 + \frac{1}{2}g_x^2 c_\epsilon^2 (|H|^2 - |H'|^2)^2 - (b'HH' + h.c.) \quad (8)$$

We can take b' to be real and positive by making a field redefinition, in which case the potential is minimized with H and H' both real and positive as well. Minimizing the potential gives the relations

$$b' = -\frac{1}{2}m_x^2 \sin(2\alpha) + \frac{1}{2} \frac{S_x}{x_H} \tan(2\alpha), \quad (9)$$

$$m_H^2 = -\frac{1}{2}m_x^2 - |\mu'|^2 + \frac{S_x}{x_H} \frac{\cos^2 \alpha}{\cos(2\alpha)}, \quad (10)$$

$$m_{H'}^2 = -\frac{1}{2}m_x^2 - |\mu'|^2 + \frac{S_x}{x_H} \frac{\sin^2 \alpha}{\cos(2\alpha)}. \quad (11)$$

Corrections to these relations from the MSSM backreaction are suppressed by powers of $\epsilon m_Z^2/m_x^2$ and can be safely neglected (away from $\tan \alpha = 1$).

3.2 Scans and Experimental Constraints

To investigate the effect of the x sector on the MSSM spectrum, we scan over this sector by choosing the values of M_x , $g_x x_H$, and ϵ at the high input scale Λ , as well as the values of S_x/x_H , m_x , $\tan \alpha$, and μ' at the lower scale $m_{3/2}$. Since the supersymmetry-breaking terms in the x sector in this scenario get direct gravity-mediated contributions, this is the natural scale for these parameters as well as for the spontaneous breakdown of $U(1)_x$, and we incorporate this property in our numerical analysis. The scan ranges considered are listed in Table 1.

A phenomenologically viable particle spectrum must have a spontaneously broken $U(1)_x$ gauge symmetry and an acceptable MSSM particle spectrum. For a given set of x -sector input values, we calculate the x - and MSSM-sector particle masses using a numerical code to integrate the modified one-loop RG equations based on Eqs. (4,5). The MSSM soft masses at the TeV scale are then put into SuSpect 2.41 [30], which calculates the physical spectrum including threshold corrections. In doing so, we also implicitly fix the values of μ and $B\mu$ to achieve electroweak symmetry breaking (EWSB) for a given value of $\tan \beta$. SuSpect also

performs a number of checks on the spectrum, such as consistent EWSB and the absence of dangerous charge or color breaking minima. Furthermore, it calculates SUSY contributions to several precision observables including the ρ parameter, the anomalous magnetic moment of the muon, and $\text{BR}(b \rightarrow s\gamma)$.

We also demand that the MSSM superpartner spectrum has a neutral lightest superpartner state (LSP), and is consistent with existing collider bounds from LEP and the Tevatron. Constraints and discovery prospects from the LHC will be discussed in more detail in Section 4. In particular, the next-to-LSP (NLSP) is typically a chargino, and the LEP bound of $m_{\chi^\pm} \gtrsim 95$ GeV [31, 32] forces $m_{3/2} \gtrsim 35$ TeV. We also impose only a very weak bound on the lightest Higgs boson mass of $m_h > 110$ GeV to allow for a theoretical uncertainty due to higher-order corrections as well as the possibility of additional contributions to its mass beyond those of the MSSM [33, 34, 35].

3.3 Viable MSSM Spectra

Upon computing the MSSM particle masses in this scenario, we find superpartner spectra that are consistent with existing experimental constraints. Most importantly, the contributions of the x sector to the MSSM can solve the tachyonic slepton problem of minimal anomaly mediation. The resulting spectra are also fairly distinctive, and could be probed in upcoming LHC searches.

The gaugino soft masses in this scenario are identical (at one loop) to their values in minimal anomaly mediation. The Wino mass M_2 is the smallest of these soft masses, followed by the Bino mass M_1 and the gluino mass M_3 . Their ratio is approximately $M_1 : M_2 : M_3 \sim 3.3 : 1.0 : 7.8$.

Scalar soft squared masses are significantly shifted by the x sector. For the first and second generations, where the Yukawa couplings can be ignored to a good approximation, the net one-loop effect can be expressed in the form

$$m_i^2(Q) = [m_i^2(Q)]_{AMSB} + Y_i^2 A + Y_i B(Q) , \quad (12)$$

where $Q < m_{3/2}$ is the RG running scale, $[m_i^2(Q)]_{AMSB}$ is the value that the soft mass would have in minimal anomaly mediation, and A and B are universal and given by (to quadratic order in ϵ)

$$A = \frac{1}{(4\pi)^2} \frac{24}{5} \left(\epsilon^2 g_1^2 |M_x|^2 \frac{1}{g_x^6 g_1^4} \right)_\Lambda \int_0^{\ln(\Lambda/m_{3/2})} dt g_x^6 g_1^4 , \quad (13)$$

$$B = \frac{1}{2} \sqrt{\frac{3}{5}} g_1^2(Q) \left(\frac{\epsilon}{g_1 g_x x_H} \right) \left(m_x^2 \cos(2\alpha) + [S_x(\Lambda)/x_H] \left[1 - \frac{g_x^2(m_{3/2})}{g_x^2(\Lambda)} \right] \right) . \quad (14)$$

The A coefficient arises from the heavy $U(1)_x$ gaugino mass and is clearly non-negative. The B coefficient can have either sign, and can be related to induced Fayet-Iliopoulos terms as discussed in Appendix A.² The soft scalar masses of the third-generation cannot be written

²Note that $\epsilon/g_x g_1$ is RG-invariant at one-loop.

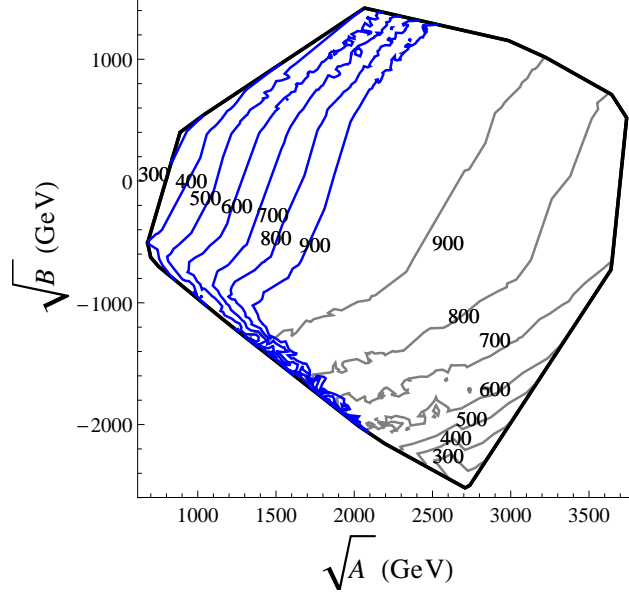


Figure 3: Lightest squark (light grey) and slepton (dark blue) masses in the phenomenologically allowed region of the A - B plane for $m_{3/2} = 60$ TeV. The lightest squarks are \tilde{b}_1, \tilde{t}_1 . The lightest sleptons are $\tilde{\nu}_\tau$ along the south-east gradient and $\tilde{\tau}_1$ along the north-east.

in such a simple form due to the effect of the larger Yukawa couplings on the RG running. Even so, the expressions in Eqs. (12,13,14) often still provide a useful approximation to their values.

It is convenient to describe the effects of the x sector on the MSSM and the corresponding phenomenologically viable regions in terms of the A and B coefficients. Indeed, any set of x -sector parameters maps onto a unique region in the A - B plane. Furthermore, it can be shown that for fixed $m_{3/2}$, any two sets of x -sector parameters that map to the same point in the A - B plane also yield identical values for the third-generation soft scalar masses and trilinear A terms [10, 36]. Therefore any point in the A - B plane corresponds to a unique MSSM spectrum in this scenario for a given value of $m_{3/2}$.

In Fig. 3 we show the allowed portion of the A - B plane for $m_{3/2} = 60$ TeV. Throughout this plane the gaugino spectrum is identical to minimal AMSB leading to nearly-degenerate Wino-like chargino and neutralino states with masses close to 165 GeV, a mostly-Bino neutralino with mass of about 545 GeV, and a 1.3 TeV gluino. Raising $m_{3/2}$ increases these masses proportionally. On the other hand, masses of the scalar superpartners vary significantly throughout the parameter region. In Fig. 3 we also show the mass contours of the lightest slepton ($\tilde{\nu}_\tau$ or $\tilde{\tau}_1$ in dark blue) and the lightest squark (\tilde{b}_1 or \tilde{t}_1 in light grey).

The allowed region in the A - B plane is cut off at small values of A by unacceptably low values of the slepton masses corresponding to $m_{L_3}^2$ and $m_{E_3^c}^2$. In particular, since $Y_L = -\frac{1}{2}$ and $Y_{E^c} = 1$, positive B values push $m_{E^c}^2$ up and m_L^2 down. Thus the region of small A with $B > 0$ is constrained by small $m_{L_3}^2$, and small A with $B < 0$ is cut off by small $m_{E_3^c}^2$. The soft

masses $m_{U_3^c}^2$ and $m_{D_3^c}^2$ also scale similarly, since $Y_{U^c} = -\frac{2}{3}$ and $Y_{D^c} = \frac{1}{3}$. Increasing A tends to increase the values of nearly all the soft scalar masses. An important exception is $m_{Q_3}^2$, which runs small due to the backreaction from the large top Yukawa contribution in its RG equation, particularly when $B < 0$. This leads to the large A region being constrained by phenomenological bounds. In the region of large A and $B < 0$, the mass difference between the light stops and sbottoms (\tilde{t}_L and \tilde{b}_L) becomes large and is constrained by the ρ parameter. For large A and $B > 0$, the up-type Higgs soft mass becomes too large and positive to allow electroweak symmetry breaking. Thus, the ρ parameter and consistent EWSB cut off the large A region for $B < 0$ and $B > 0$ respectively.

The allowed region in Fig. 3 also shows that we need $\sqrt{|B|} \lesssim \sqrt{A}$ to obtain a viable MSSM spectrum. Since the B coefficient goes like $g_1 g_x \epsilon m_{3/2}^2 \ln(\Lambda/m_{3/2})$ while A goes like $g_1^2 \epsilon^2 m_{3/2}^2 \ln(\Lambda/m_{3/2})$, the natural size of A relative to B is down by a factor of $(\epsilon/g_1 g_x) g_1^2(Q)$. Thus, a mild cancellation is usually needed between the two contributions to B to keep it relatively small, corresponding to a fine tuning on the order of ϵ . From this point of view, slightly larger values of ϵ are favourable.

3.4 Mass Sum Rules

The scalar superpartner masses vary widely over the A - B plane, and the third generation squarks can be significantly lighter than those of the first two. We will discuss their spectrum in more detail below. Despite this variation, the scalar superpartner masses of the first two generations satisfy a set of simple sum rules related to the A - B parametrization described above.

Only one field, E^c , has hypercharge such that $Y = Y^2$, so at least three soft masses are needed to eliminate *both* A and B . Up to an overall normalization, the complete set of soft mass combinations that are independent of the x sector is then given in Table 2 including the predictions from our model; these depend only on the standard AMSB expressions for the soft masses [1, 2].

Note that the ordinary AMSB soft masses depend only on the three gauge couplings and $m_{3/2}$. However, the dependence on the $U(1)_x$ gauge coupling is in all cases proportional to Y^2 ; this is the same as the dependence on A , so g_1 will cancel by construction from the functions we have considered. All the masses depend on $m_{3/2}$ identically, and so only two of the ten combinations are linearly independent. This can be seen clearly in the second column of Table 2.

While the values of the sum rules are independent of the x sector, the ones that will be most useful in practice are not. The spectrum will determine which three scalar masses can be measured first, and thus compared to the predictions of Table 2. The question of the extent to which these predictions can be tested at the LHC or other possible future experiments is deferred to future work.

Scalar Mass Sum Rule	Prediction	
	Analytic $\times \frac{m_{3/2}^2}{(4\pi)^4}$	Numerical
$24m_Q^2 + m_u^2 - 10m_d^2$	$120g_3^4 - 36g_2^4$	$(4.8 \text{ TeV})^2$
$3m_Q^2 - 3m_u^2 + 5m_L^2$	$-12g_2^4$	$-(550 \text{ GeV})^2$
$24m_Q^2 + 3m_u^2 - 2m_e^2$	$216g_3^4 - 36g_2^4$	$(6.5 \text{ TeV})^2$
$15m_Q^2 - 6m_d^2 + m_L^2$	$72g_3^4 - 24g_2^4$	$(3.7 \text{ TeV})^2$
$24m_Q^2 - 15m_d^2 + m_e^2$	$72g_3^4 - 36g_2^4$	$(3.7 \text{ TeV})^2$
$27m_Q^2 + 5m_L^2 - 2m_e^2$	$216g_3^4 - 48g_2^4$	$(6.5 \text{ TeV})^2$
$5m_u^2 - 2m_d^2 - 8m_L^2$	$24g_3^4 + 12g_2^4$	$(2.3 \text{ TeV})^2$
$m_u^2 + 5m_d^2 - m_e^2$	$48g_3^4$	$(3.1 \text{ TeV})^2$
$27m_u^2 - 40m_L^2 - 2m_e^2$	$216g_3^4 + 60g_2^4$	$(6.7 \text{ TeV})^2$
$27m_d^2 + 8m_L^2 - 5m_e^2$	$216g_3^4 - 12g_2^4$	$(6.4 \text{ TeV})^2$

Table 2: The ten combinations of squark and slepton masses that are independent of the details of the x sector, and the predictions for those values ($m_{3/2} = 60 \text{ TeV}$).

4 Phenomenology

The modified AMSB scenario under consideration has gaugino masses as in minimal AMSB together with a broad range of scalar soft masses that can be characterized by the two parameters A and B . In this section we investigate the collider and cosmological implications of the resulting superpartner spectra. A key feature of the spectra is that the LSP is almost always a predominantly Wino neutralino accompanied by a nearly degenerate chargino state. The small mass difference makes the chargino metastable and allows it travel a macroscopic distance (typically a few cm) before decaying. We begin by discussing the implications of this effect on the collider signals of this scenario. Next, we study the mass spectrum and the LHC collider phenomenology of several specific benchmark points within the A - B plane, which we find can be significantly different from those considered in other modified AMSB scenarios [37, 38, 39, 40]. Finally, we comment on the effects of a mostly-wino LSP on cosmology.

4.1 Charginos and Charged Tracks

As in minimal AMSB, the gaugino mass spectrum in our scenario has a Wino that is considerably lighter than the other gauginos. In most of the parameter space the μ term is also much larger than M_2 . These two features lead to a chargino NLSP that is nearly degenerate with a mostly-Wino neutralino LSP. If the mass splitting exceeds the charged pion mass $\Delta m > m_\pi$, the dominant decay mode is $\tilde{\chi}_1^\pm \rightarrow \tilde{\chi}_1^0 \pi^\pm$. The rate for this decay is often quite slow and the chargino can travel a macroscopic distance to produce a charged track several centimeters long [26, 41, 42]. If $\Delta m < m_\pi$, the even slower three-body mode $\tilde{\chi}_1^\pm \rightarrow \tilde{\chi}_1^0 e \nu_e$ dominates and gives rise to a long charged track that extends beyond the muon chamber [43]. Such long-lived charginos could be seen in standard searches for metastable charged particles. On the other hand, short charged track stubs from the two-body decay

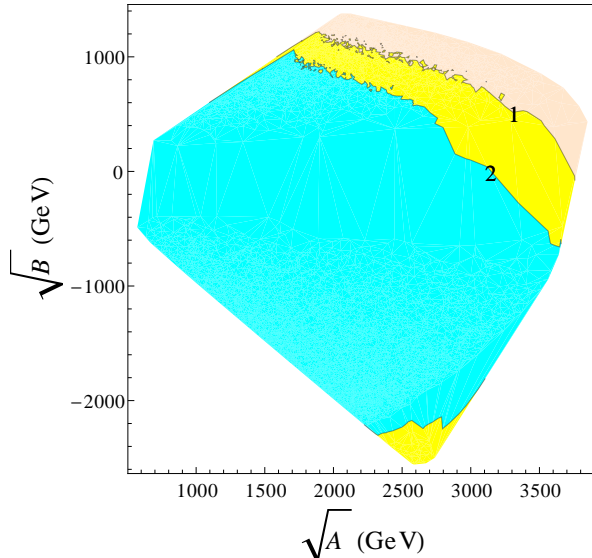


Figure 4: Chargino decay lengths $c\tau$ in cm throughout the A - B plane for $m_{3/2} = 60$ TeV and $\tan\beta = 10$.

require a different set of triggers, as discussed in Ref. [44].

Evidently the chargino-neutralino mass difference plays a crucial role in determining the collider phenomenology of this and other AMSB-like constructions. Relative to minimal AMSB, the value of μ (as determined by electroweak symmetry breaking and the predicted scalar soft masses) and the masses of the scalar superpartners can be considerably different in our scenario, and this can modify the chargino-neutralino mass difference. In most of the A - B plane we find that μ is very large relative to M_2 leading to a very small tree-level mass splitting Δm , typically well below the pion mass. However, as discussed in Ref. [26], finite loop corrections involving the scalar superpartners tend to increase the mass splitting above the pion threshold [45].

We find that one-loop corrections to the MSSM spectrum push $\Delta m > m_\pi$ throughout the entire A - B plane for any reasonable values of $m_{3/2}$ and $\tan\beta$ [26]. This leads to dominant two-body chargino decays with decay lengths $c\tau$ in the range of a few centimeters, as illustrated in Fig. 4 for $m_{3/2} = 60$ TeV and $\tan\beta = 10$. The mass splitting is largest towards the upper-right section of this plane due to smaller values of μ that occur there. Additionally, light mostly left-handed stops and sbottoms increase the mass splitting in the bottom-right section of the plane.

Charged track stubs of this length could be observed in the inner detectors of ATLAS and CMS, albeit with some difficulty. Without a dedicated search for them, the light charginos contribute to missing energy in the event since the pion emitted in their decay is very soft. As such, the standard SUSY search techniques can be applied to this scenario as well, and we will treat both states as contributing to missing energy for the remainder of this discussion. However, the track stubs from chargino decays could potentially be extracted from the inner detector if a specific search is made for them, provided they are accompanied by a hard jet

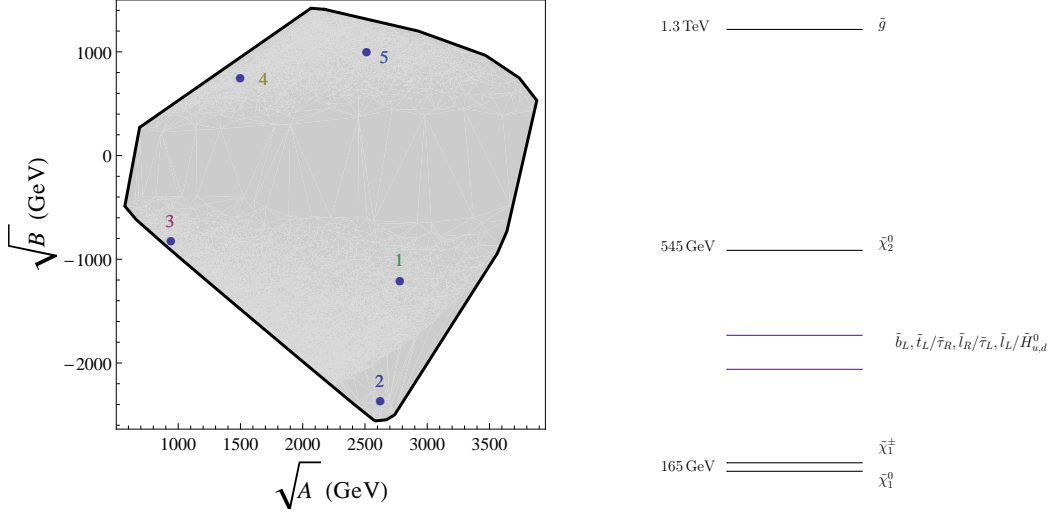


Figure 5: Locations of the five benchmark points in the A - B plane with $m_{3/2} = 60$ TeV (left), and the schematic particle spectrum of these points (right).

or photon to serve as a trigger [26, 38, 39, 46].

4.2 Benchmark Points

We study five benchmark points that cover a broad range of the qualitative collider signatures that can arise in this scenario. Recall from Fig. 3 that the left-handed squark soft masses increase from lower right to upper left in the A - B plane, the right-handed slepton soft masses increase from upper left to lower right, and the left-handed slepton soft masses increase from lower left to upper right. Our benchmark points are chosen along these three gradients, and we show their locations in the A - B plane in the left panel of Fig. 5. For all these points, we choose $m_{3/2} = 60$ TeV and $\tan \beta = 10$, and we label them as XAMSB $_i$ with $i = 1 - 5$. Our choice of $m_{3/2}$ provides a superpartner spectrum that is accessible at the LHC while being consistent with existing LHC searches.

For each benchmark point we generate decay tables using SUSY-HIT [47]. The leading-order LHC7 production cross sections (pp collider at $\sqrt{s} = 7$ TeV) are computed with Pythia 6.4 [48]. We also cross-check our results with BRIDGE [49] and MadGraph [50], and find consistent behaviour. The generic features of the spectra for all these points are illustrated schematically in the right panel of Fig. 5. The mass spectra and dominant branching fractions are shown in Figs. 6-8, while the leading superpartner production cross sections at the LHC are listed in Tables 3, 4, 5. In Figs. 6-8, the notation for branching ratios to NLSP/LSP is in the order of heavier/lighter SUSY final state.

All these points have similar gaugino spectra, with a mostly-Wino LSP and chargino NLSP with masses close to 165 GeV, a mostly-Bino neutralino with mass near 545 GeV, and a gluino with mass near 1.3 TeV. On the other hand, the masses of Higgsino-like states

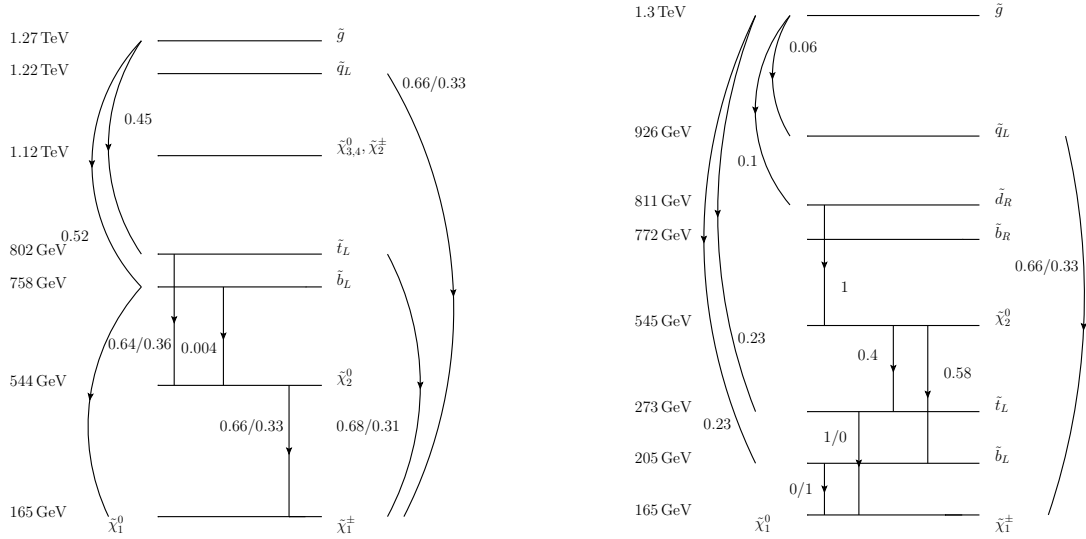


Figure 6: Mass spectrum and decay branching fractions for the benchmark points $XAMSB_1$ (left) and $XAMSB_2$ (right).

σ_{SUSY}	1.35 pb	σ_{SUSY}	8.55 pb
$\tilde{\chi}_1^0 \tilde{\chi}_1^\pm + \tilde{\chi}_1^\mp \tilde{\chi}_1^\pm$	1.34 pb	$\tilde{\chi}_1^0 \tilde{\chi}_1^\pm + \tilde{\chi}_1^\mp \tilde{\chi}_1^\pm$	1.25 pb
$\tilde{q}_L \tilde{q}_L^{(*)}$	2.4 fb	$\tilde{b}_1 \tilde{b}_1$	6.0 pb
$\tilde{\chi}_1^0 \tilde{q}_L + \tilde{\chi}_1^\pm \tilde{q}_L$	1.36 fb	$\tilde{t}_1 \tilde{t}_1$	1.2 pb
$\tilde{g} \tilde{q}_L$	1.2 fb	$\tilde{q}_L \tilde{\chi}_1^0$	0.09 pb
$\tilde{g} \tilde{g}$	0.1 fb	$\tilde{q}_L \tilde{q}_L^{(*)}$	0.02 pb
$\tilde{b}_L \tilde{b}_L^{(*)}$	0.9 fb	$\tilde{q}_L \tilde{q}_R$	7.0 fb
$\tilde{t}_L \tilde{t}_L^{(*)}$	0.7 fb	$\tilde{d}_R \tilde{d}_R^{(*)}$	0.3 fb

Table 3: Production cross sections for $XAMSB_1$ and $XAMSB_2$.

as well as the scalar spectra vary widely. We will discuss the details below.

4.2.1 $XAMSB_1$ ($\sqrt{A} = 2775$ GeV, $\text{sgn}\sqrt{B} = -1203$ GeV)

The $XAMSB_1$ benchmark point has a mostly left-handed sbottom with a mass near 750 GeV and a slightly heavier left-handed stop near 800 GeV as the lightest squarks. The other squarks and the gluino have masses in excess of 1.2 TeV, as seen in the left panel of Fig. 6.

The production of superpartners is dominated by electroweak chargino and neutralino pair creation processes, and is given in Table 3. The lightest neutralino will be invisible, as will the lightest chargino up to an accompanying short charged track stub and a very soft pion. To observe these electroweak production processes, an additional radiated hard jet or photon would be required [38, 39, 46]. The associated squark/-ino production modes would yield a similar monojet signal, but have very small cross sections (given in Table 3).

σ_{SUSY}	1.35 pb	σ_{SUSY}	1.4 pb
$\tilde{\chi}_1^0 \tilde{\chi}_1^\pm + \tilde{\chi}_1^\mp \tilde{\chi}_1^\pm$	1.33 pb	$\tilde{\chi}_1^0 \tilde{\chi}_1^\pm + \tilde{\chi}_1^\mp \tilde{\chi}_1^\pm$	1.39 pb
$\tilde{q}_L \tilde{q}_L$	2.8 fb	$\tilde{q}_L \tilde{q}_L$	1.6 fb
$\tilde{q}_L \tilde{\chi}_1^\pm$	1.5 fb	$\tilde{q}_R \tilde{q}_R$	0.35 fb
$\tilde{q}_R \tilde{q}_R$	0.7 fb	$\tilde{q}_R \tilde{g}$	0.3 fb

Table 4: SUSY production cross section for $XAMSB_3$ and $XAMSB_4$

The rates for QCD production of squarks and gluinos are suppressed by the heavier masses of these states. For the gluino and the light-flavour squarks, the production rates are safely below the current limits from LHC searches for jets and missing energy (MET) [51, 52, 53, 54]. This is also true for the lighter stop and sbottom states, which have lower production rates for a given mass since they are not created efficiently via $q\bar{q}$ initial states. In particular, the sbottom and stop states are heavy enough to avoid the LHC limits from searches for b jets and MET [55] as well as inclusive searches for jets and MET.

4.2.2 $XAMSB_2$ ($\sqrt{A} = 2617$ GeV, $\text{sgn}\sqrt{B} = -2364$ GeV)

The spectrum for $XAMSB_2$ has a mostly left-handed sbottom and stop that are light relative to the other squarks. As shown in Table 3, this leads to very large production cross-sections. The smaller mass differences between these squarks and the Wino-like chargino and neutralino states cause them to decay primarily into b quarks and $\tilde{\chi}_1^0$ (for \tilde{b}_1) or $\tilde{\chi}_1^+$ (for \tilde{t}_1) rather than the kinematically-suppressed top modes. As such, we expect that this point can be probed by LHC searches in the inclusive jets plus MET channels [51, 52, 53, 54], in addition to searches for bottom jets and MET [55]. However, despite the large production rates the relatively small mass differences between the stop/sbottom and the chargino/neutralino make these squarks difficult to detect. For this reason, these states are not constrained by Tevatron searches [56, 57], and we expect the same to hold for existing LHC searches.

The \tilde{d}_R state is also not overly heavy at the $XAMSB_2$ sample point. Its production is too small to be observed with existing analyses. Even so, with future searches in mind we note that it decays through an extended cascade, going first to $d + \tilde{\chi}_2^0$, followed by $\tilde{\chi}_2^0$ decaying to $\tilde{t}_L + t$ or $\tilde{b}_L + b$, which then go to $b + (N)LSP$. The net final state therefore consists of multiple light and b jets, possibly some leptons, and missing energy.

4.2.3 $XAMSB_3$ and $XAMSB_4$

($\sqrt{A} = 938$ GeV, $\text{sgn}\sqrt{B} = -809$ GeV) and ($\sqrt{A} = 1491$ GeV, $\text{sgn}\sqrt{B} = 749$ GeV)

Points $XAMSB_3$ and $XAMSB_4$ are similar in that they both have relatively light sleptons, lighter than the mostly-Bino state, as can be seen in Fig. 7. In the case of $XAMSB_3$ the lighter sleptons are mainly right-handed, while for $XAMSB_4$ they are predominantly left-handed. The presence of such light sleptons offers the possibility of additional leptons in

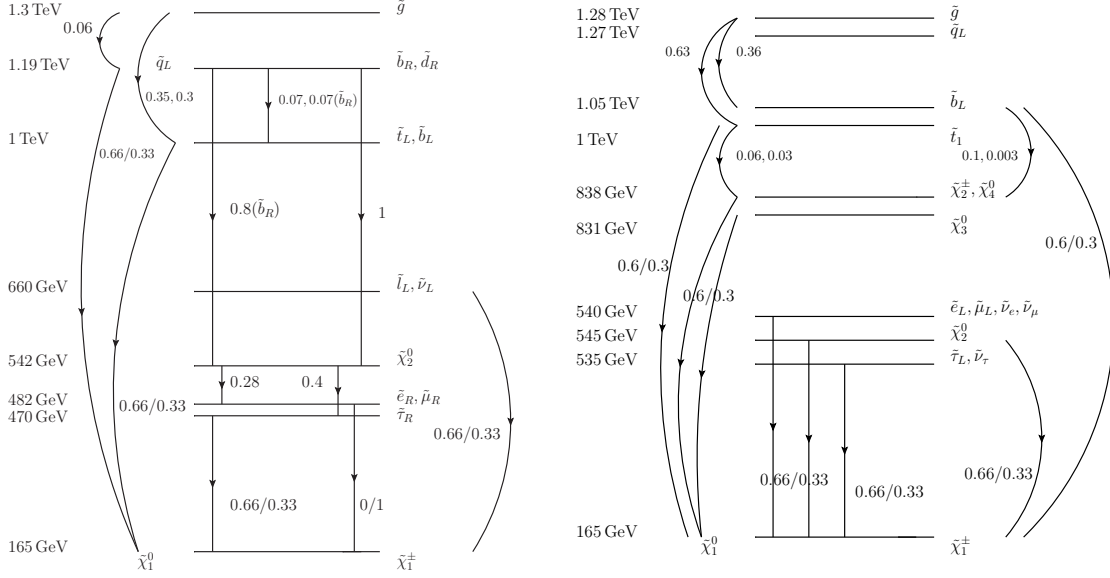


Figure 7: Spectrum and branching fractions for $XAMSB_3$ and $XAMSB_4$.

cascade decays. Both points also have all squarks heavier than about 1 TeV, and are therefore expected to be consistent with existing LHC searches for jets plus MET.

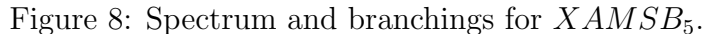
The mass spectrum of $XAMSB_3$ leads to final states with multiple leptons. The right-handed squarks decay preferentially to the Bino-like $\tilde{\chi}_2^0$ neutralino rather than the lighter Wino-like neutralinos and charginos. Subsequently, $\tilde{\chi}_2^0$ decays most of the time to the lighter charged sleptons by emitting the corresponding charged lepton. Yet another charged lepton (of opposite sign) will be produced if the slepton decays to the neutralino LSP. The dilepton invariant mass in this case will provide an efficient probe of the underlying slepton masses.

In contrast, the relatively light (mostly left-handed) sleptons of $XAMSB_4$ are not populated very efficiently by cascade decays. The $\tilde{\chi}_2^0$ mode decays primarily via a W^\pm or Z^0 in a 2:1 ratio to $\tilde{\chi}_1^\pm$ or $\tilde{\chi}_1^0$, and are therefore a less efficient source of leptons. The most promising search strategy for this parameter point is thus likely to be jets plus MET.

4.2.4 $XAMSB_5$ ($\sqrt{A} = 2506$ GeV, $sgn\sqrt{B} = 1004$ GeV)

Relative to the other sample points, the distinctive feature of $XAMSB_5$ is that it has lighter higgsinos. As shown in Fig. 8, these give rise to multiple chargino and neutralino states with masses close to 600 GeV, well below the masses of all the scalars. In comparison, the lightest squarks are the mostly-left-handed stop and sbottom, with masses close to 1 TeV.

The lighter stop and sbottom states have significant branching fractions to decay to Higgsino-like charginos or neutralinos, on account of the large top Yukawa coupling. Their

Table 5: SUSY production cross sections for $XAMS B_5$

4.3 Comments on Dark Matter

³ Note as well that the metastable charginos decay relatively quickly on cosmological time scales, and certainly well before the onset of primordial nucleosynthesis.

obtained, but the entire superpartner mass spectrum in this case is very heavy relative to the electroweak scale.

An acceptable mostly-Wino neutralino relic density can arise for smaller neutralino masses if these states are produced non-thermally, such as through the decay of a moduli field [59, 60]. Due to the relatively large annihilation cross section of such states, they have been put forward [61, 62] as a possible explanation for the apparent excess of positrons seen by the PAMELA experiment [63]. However, this proposal is constrained by the apparent absence of an excess in antiproton cosmic rays in the PAMELA data [64], by searches by the Fermi Space Telescope for gamma rays that are monoenergetic [65] or originating in dwarf spheroidal galaxies [66], and from limits on energy injection at recombination based on measurements of the cosmic microwave background [67]. Mostly-Wino DM can also be consistent with existing bounds from direct detection (such as XENON 100 [68]) provided $|M_2/\mu| \ll 1$ [59, 40].

5 Conclusion

In this work we have proposed and investigated a simple extension of minimal AMSB that can give rise to a viable spectrum of MSSM superpartners while not introducing dangerous new sources of flavour mixing. A sequestered MSSM sector couples via a gauge kinetic mixing coupling of hypercharge to a new, unsequestered $U(1)_x$ gauge multiplet.

We find that the new gauge multiplet provides an additional source of supersymmetry breaking that can render all MSSM squark and slepton soft masses positive and produce a phenomenologically viable spectrum. The gaugino masses in this scenario are nearly identical to those in minimal AMSB, while the scalar masses cover a diverse range of values.

The LSP in this scenario is a mostly-Wino neutralino that is nearly degenerate in mass with a mostly-Wino chargino. This chargino can travel a macroscopic distance of a few centimeters after being produced in a high-energy collider, giving rise to charged track stubs. The scalar spectrum in this scenario tends to yield top- and bottom-rich cascade decays at the LHC together with missing energy. Multi-lepton states can arise in certain cases as well. Measuring the masses of a variety of these states could help to identify this scenario using LHC data as the soft scalar masses satisfy a number of simple sum rules.

Acknowledgements

We thank Thomas Grégoire, John Ng, Robert McPherson, David Poland, Yael Shadmi, and Scott Watson for helpful discussions. DM would also like to thank the CERN theory group for their hospitality while this work was being completed. This research was supported by the National Sciences and Engineering Research Council of Canada (NSERC).

A Soft Masses and RG Running

The effects of the x sector on the RG running of the MSSM soft masses can be derived in a simple way by using analytic continuation methods in superspace [69, 70]. For this, it is convenient to describe the approximately globally supersymmetric theory valid below Λ with a renormalized 1PI effective Lagrangian of the form

$$\begin{aligned} \mathcal{L} = & \int d^4\theta \left(Z_i \phi_i^\dagger e^{2Y_i V_Y} \phi_i + Z_p H_p^\dagger e^{2x_p V_x} H_p \right) + \left(\int d^2\theta W + h.c. \right) \\ & + \int d^4\theta (\xi_Y V_Y + \xi_x V_x) + \int d^2\theta \left(\frac{1}{4G_Y^2} B^\alpha B_\alpha + \frac{1}{4G_x^2} X^\alpha X_\alpha + \frac{\epsilon_h}{2} X^\alpha B_\alpha \right) + (h.c.) . \end{aligned} \quad (15)$$

Soft supersymmetry breaking is contained within non-vanishing auxiliary components of the renormalized couplings, which are now elevated to real (Z_i) and chiral (G_i, ϵ_h) superfields. The θ^4 component of $\ln Z_i$ contributes to the soft scalar squared mass of ϕ_i ,

$$\Delta m_i^2 = -\ln Z_i|_{\theta^4} , \quad (16)$$

while a trilinear A -term of the form $\phi_i \phi_j \phi_k$ comes from

$$A_{ijk} = (\ln Z_i + \ln Z_j + \ln Z_k)|_{\theta^2} . \quad (17)$$

In the gauge sector, we identify the physical gauge coupling and gaugino mass with a real superfield R given by

$$R_a \equiv \frac{1}{2G_a^2} + \frac{1}{2G_a^{2\dagger}} - \sum_i \frac{q_i^2}{8\pi^2} \ln Z_i + \dots , \quad (18)$$

with the sum running over all fields with charge q_i under the a -th gauge group and the omitted terms are of higher order in the gauge coupling. From this vector superfield, we obtain the physical gauge coupling and gaugino mass according to

$$R_a|_0 = \frac{1}{g_a^2}, \quad R_a|_{\theta^2} = -\frac{M_a}{g_a^2} . \quad (19)$$

The θ^4 component of R_a is smaller by a loop factor [70].

In the same way, we can form a real superfield E corresponding to ϵ_h :

$$E = \frac{\epsilon_h + \epsilon_h^\dagger}{2} - \sum_i \frac{q_{ix} q_{iY}}{8\pi^2} \ln Z_i + \dots \quad (20)$$

With this prescription, we identify the physical kinetic mixing parameter ϵ with

$$\epsilon = E / \sqrt{R_x R_Y}|_0 \simeq g_x g_Y \text{Re}(\epsilon_h) . \quad (21)$$

The holomorphic basis of Eq. (15) is useful because it separates the running of hypercharge and $U(1)_x$. Holomorphy implies that the running of G_x , G_Y , and ϵ_h is one-loop exact. For the gauge couplings,

$$\frac{d}{dt} \left(\frac{1}{G_a^2} \right) = \frac{b_a}{8\pi^2}, \quad b_a = -\text{tr}(q_i^2) = -2x_H^2, \quad -33/5 . \quad (22)$$

Taking the θ^2 component of Eq. (22) then gives the standard MSSM one-loop RG equation for M_1 as well as

$$(4\pi)^2 \frac{dM_x}{dt} = 4x_H^2 g_x^2 M_x . \quad (23)$$

Since there are no fields in the low-energy theory charged under both hypercharge and $U(1)_x$, the holomorphic mixing ϵ_h does not run at all [71]. As long as the source of kinetic mixing is sequestered from supersymmetry breaking, ϵ_h has a vanishing θ^2 component and there is no mixed gaugino soft mass in this basis. We also have to one-loop order

$$\frac{d\epsilon}{dt} \simeq \left(\frac{\beta_x}{g_x} + \frac{\beta_Y}{g_Y} \right) \epsilon \simeq \frac{1}{4\pi^2} \left(2x_H^2 g_x^2 + \frac{33}{5} g_1^2 \right) \epsilon , \quad (24)$$

with $\beta_a = dg_a/dt$.

Running of the soft scalar squared masses and the trilinear A terms can be derived from the higher components of the wavefunction factors. At one-loop order, the running of the wavefunction of the i -th MSSM field is [71]

$$(4\pi^2) \frac{d \ln Z_i}{dt} = (4\pi^2) \left(\frac{d \ln Z_i}{dt} \right)_{MSSM} + 4Y_i^2 R_Y^{-1} \left(\frac{1}{1 - E^2 R_x^{-1} R_Y^{-1}} - 1 \right) , \quad (25)$$

where the E^2 -dependent correction comes from resumming double insertions of the kinetic mixing on diagrams of the form of Fig. 2. Expanding out the correction to quadratic order in ϵ gives

$$(\dots)|_{\theta^2} = 4g_Y^2 Y_i^2 \epsilon^2 (M_x + 2M_1) , \quad (26)$$

$$(\dots)|_{\theta^4} = 8g_Y^2 Y_i^2 \epsilon^2 (|M_x + M_1|^2 + 2|M_1|^2) . \quad (27)$$

Keeping only those terms that are enhanced by $|M_x| \gg |M_1|$ leads to the M_x -dependent parts of Eqs. (4,5).

The Lagrangian of Eq. (15) also contains Fayet-Iliopoulos (FI) terms for $U(1)_x$ and hypercharge. At one-loop they run according to [36]

$$\frac{d\xi_a}{dt} = \frac{2}{(4\pi)^2} \text{tr}(q_a \Delta m^2) , \quad (28)$$

where Δm_i^2 is the contribution to the i -th scalar soft mass from the corresponding wavefunction factor, as in Eq. (16). For a single $U(1)$ factor, when the auxiliary D -fields are integrated out, the FI terms effectively contribute to the scalar soft masses, producing a total value of

$$m_i^2 = \Delta m_i^2 + q_{i,a} g_a^2 \xi_a . \quad (29)$$

The RG running of these two contributions can be dealt with separately, or together in a single RG equation for m_i^2 . In the latter case, the contributions of the FI term to the running are closely related to the “S” terms proportional to $\text{tr}(Y m^2)$ that appear in the

usual RG equations for the MSSM soft scalar masses [72]. With several $U(1)$ factors and kinetic mixing, there are additional effects that we will describe below.

After running from the high scale Λ in the $\text{MSSM} \times U(1)_x$ theory down to scale $m_{3/2}$, we integrate out the x sector and continue to run the remaining soft masses in the MSSM alone. For this, it is convenient to convert Eq. (15) to a canonical basis for all fields, as in Eq. (2). Kinetic mixing among the gauge fields and the gauginos can be eliminated by shifting the (now canonically normalized aside from the mixing) vector multiplets according to

$$\begin{aligned} V_Y &\rightarrow V_Y - s_\epsilon V_x, \\ V_x &\rightarrow c_\epsilon V_x, \end{aligned} \quad (30)$$

where $c_\epsilon = 1/\sqrt{1-\epsilon^2}$ and $s_\epsilon = \epsilon c_\epsilon$. After making this shift, the vector multiplets are canonically normalized with no gauge kinetic mixing, the fields initially charged under $U(1)_x$ now couple to the $U(1)_x$ multiplet with strength

$$g_x c_\epsilon x_p \equiv \tilde{g}_x x_p. \quad (31)$$

In particular, the mass of the $U(1)_x$ vector boson is $2\tilde{g}_x^2 x_H^2 \eta^2$, where $\eta = \sqrt{\langle H \rangle^2 + \langle H' \rangle^2}$. Those fields initially charged only under hypercharge now couple in the same way as before to the $U(1)_Y$ multiplet, but they also develop a coupling to the $U(1)_x$ multiplet of strength

$$- \tilde{g}_x s_\epsilon \left(\frac{g_Y}{\tilde{g}_x} \right) Y_i. \quad (32)$$

This shift induces a small amount of mass mixing among the vector and gaugino fields. For the vectors, the mixing is on the order of $\epsilon^2 m_Z^2 / m_x^2$ while for the gauginos it is $\epsilon M_1 / M_x$. We neglect this effect since it is suppressed by both a small mass ratio and the kinetic mixing parameter.

Shifting the gauge multiplets also modifies the hypercharge and $U(1)_x$ D terms. The D -term potential becomes

$$\begin{aligned} V_D = & \frac{1}{2} c_\epsilon^2 g_x^2 \left(\sum_i x_i |H_i|^2 \right)^2 + c_\epsilon^2 (g_x^2 \xi_x - \epsilon g_x g_Y \xi_Y) \sum_i x_i |H_i|^2 \\ & + \frac{1}{2} c_\epsilon^2 g_Y^2 \left(\sum_i Y_i |\phi_i|^2 \right)^2 + c_\epsilon^2 \left[g_Y^2 \xi_Y - \epsilon g_x g_Y \left(\sum_i x_i |H_i|^2 + \xi_x \right) \right] \sum_i Y_i |\phi_i|^2. \end{aligned} \quad (33)$$

The terms quadratic in the scalar fields can be absorbed as shifts in the soft squared masses. From this, we see that kinetic mixing alters the effective MSSM soft masses through both the $U(1)_x$ FI term and the VEVs of H and H' . Using Eqs. (28,29), the explicit dependence on FI terms can be incorporated instead into the running of the total scalar soft masses in both the visible and the x sector. This is the origin of the term proportional to $S_x = x_H(m_H^2 - m_{H'}^2)$ in Eq. (4) [36]. Incorporating the FI terms into the running of the x -sector total soft masses, we find

$$(4\pi)^2 \frac{dm_{H,H'}^2}{dt} = -8x_H^2 g_x^2 |M_x|^2 \pm 2\tilde{g}_x^2 x_H^2 (m_H^2 - m_{H'}^2) \mp 2s_\epsilon \sqrt{\frac{3}{5}} x_H \tilde{g}_x g_1 \text{tr}(Y m^2). \quad (34)$$

Parameter	Interval
m_H^2	$[-100, 100]$
$m_{H'}^2$	$[-100, 100]$
b'	$[0, 100]$
μ'	$[-10, 10]$

Table 6: Scan range of Lagrangian parameters for exploration of fine tuning in the x sector. Note that the overall scale of these parameters is unimportant to this appendix.

From Eq. (33) we see as well that in integrating out the massive x -sector at scale $m_{3/2}$, the effective MSSM soft masses are shifted by

$$m_i^2 \rightarrow m_i^2 + \frac{s_\epsilon}{2} \frac{Y_i}{x_H} \frac{g_Y}{\tilde{g}_x} m_x^2 \cos 2\alpha , \quad (35)$$

which coincides with the prescription of Eq. (7).

B Fine Tuning in the Scalar Potential

The x -sector scalar potential has a D -flat direction when the two Higgs states have equal expectation values. In this case, the potential of Eq. (8) is purely quadratic and can not have a stable non-zero minimum. The requirement that the quadratic coefficient in the D -flat direction is positive also disfavors a minimum with $\tan \alpha$ close to unity when this parameter is determined from a uniform scan over the soft supersymmetry breaking parameters in the x sector; it requires a fine tuning to make the combination $m_H^2 + m_{H'}^2 + 2\mu'^2 - 2b$ much smaller than the natural scale, $m_{3/2}^2$. For this reason, in our parameter scans discussed in Section 3 where we use a uniform prior on $\tan \alpha$, we excise a small region around $\tan \alpha = 1$.

To quantify this fine tuning, we perform a simple scan over the Lagrangian parameters to answer two questions: what is the implied distribution of $\tan \alpha$ for flat priors on the x -sector supersymmetry breaking parameters; and when do we get an “unnatural” cancellation between the Lagrangian parameters, leading to very light states. As the overall scale is unimportant, we treat the mass parameters as dimensionless and use flat priors with the ranges given in Table 6. Note that we may choose b' positive without loss of generality. We randomly generate 10^6 points, rejecting those where the potential is not bounded from below or the $U(1)_x$ gauge symmetry is not spontaneously broken. For the survivors we calculate both $\tan \alpha$ and the mass of the lightest bosonic state, the lighter real scalar.

We plot the (unnormalised) distribution of $\tan \alpha$ in Fig. 9. The general behaviour is easy to understand. Recall that α is given by

$$\sin(2\alpha) = \frac{2b'}{m_H^2 + m_{H'}^2 + 2\mu'^2}. \quad (36)$$

Uniform priors on the Lagrangian parameters would lead to an approximately flat distribution in $\sin(2\alpha)$. Demanding spontaneous symmetry breaking as well imposes a lower limit

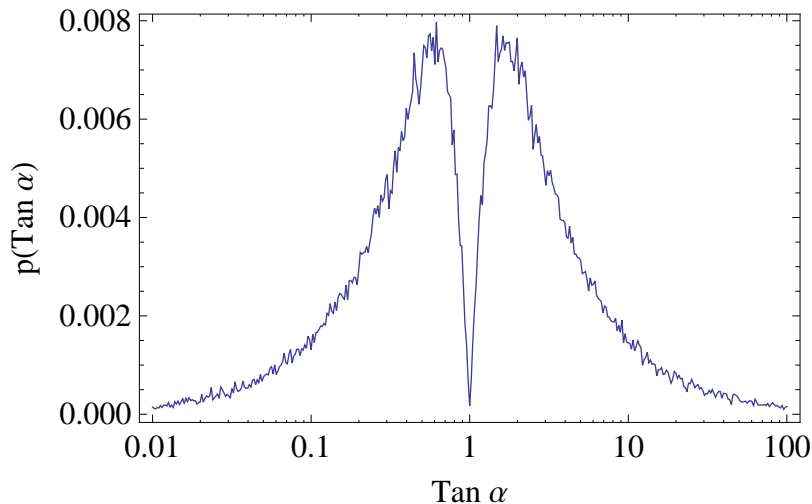


Figure 9: Distribution of $\tan \alpha$ implied by uniform priors on Lagrangian parameters, and imposing consistent spontaneous symmetry breaking.

on b' , and thus biases $\sin(2\alpha)$ – and hence also $\tan \alpha$ – towards unity. The dip in Fig 9 at $\tan \alpha = 1$ is due to the Jacobian of the variable transformation:

$$p(\tan \alpha) = \left| \frac{d \sin(2\alpha)}{d \tan \alpha} \right| \bar{p}(\sin(2\alpha)) = \frac{|1 - \tan^2 \alpha|}{(1 + \tan^2 \alpha)^2} \bar{p}(\sin(2\alpha)). \quad (37)$$

We see that $\tan \alpha$ very close to unity is thus theoretically disfavoured.

Further, small values of $|\tan \alpha - 1|$ are atypical in another sense. In Fig. 10 we show the fraction of points for a given $\tan \alpha$ for which the mass of the lightest scalar is one-tenth or less of the average of the Lagrangian parameters:

$$m_{h_{1x}}^2 \leq 10^{-2} \times \frac{1}{4} (|m_H^2| + |m_{H'}^2| + \mu'^2 + b'). \quad (38)$$

This corresponds to a 1% cancellation that is unprotected by any symmetries. It is clear that these points are almost exclusively associated with $\tan \alpha$ close to 1. They correspond to the near-flatness of the potential for $|\tan \alpha - 1| \ll 1$, and they also coincide with very large vector boson masses $m_x^2 \gg m_{3/2}^2$. In our phenomenological analysis in Section 3 where we scan over $\tan \alpha$ with a uniform prior, we exclude this unlikely central peak by demanding $|\tan \alpha - 1| > 0.1$.

References

- [1] L. Randall and R. Sundrum, *Out of this world supersymmetry breaking*, *Nucl. Phys.* **B557** (1999) 79–118, [[hep-th/9810155](#)].
- [2] G. F. Giudice, M. A. Luty, H. Murayama, and R. Rattazzi, *Gaugino Mass without Singlets*, *JHEP* **12** (1998) 027, [[hep-ph/9810442](#)].

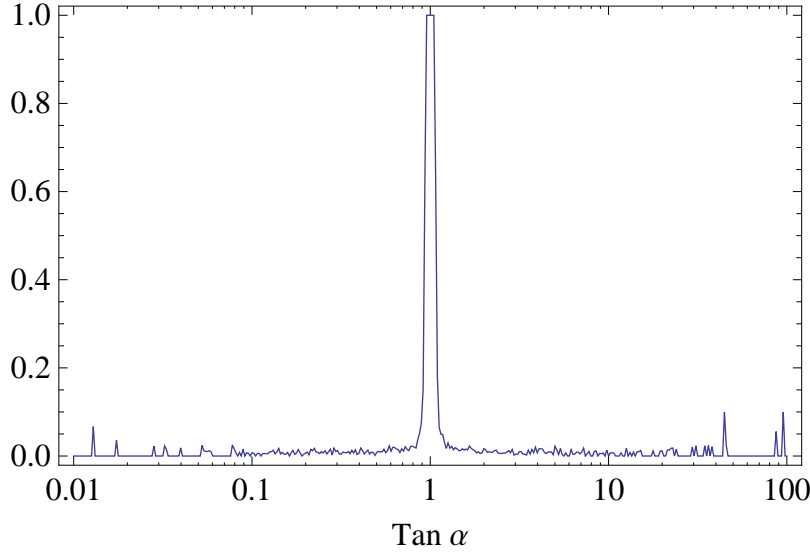


Figure 10: Fraction of points with scalars lighter than one-tenth the mean Lagrangian parameters, as a function of $\tan \alpha$.

- [3] A. Pomarol and R. Rattazzi, *Sparticle masses from the superconformal anomaly*, *JHEP* **05** (1999) 013, [[hep-ph/9903448](#)].
- [4] E. Katz, Y. Shadmi, and Y. Shirman, *Heavy thresholds, slepton masses and the μ term in anomaly mediated supersymmetry breaking*, *JHEP* **08** (1999) 015, [[hep-ph/9906296](#)].
- [5] R. Sundrum, *'Gaugomality' mediated SUSY breaking and conformal sequestering*, *Phys. Rev.* **D71** (2005) 085003, [[hep-th/0406012](#)].
- [6] Y. Cai and M. A. Luty, *Minimal Gaugomality Mediation*, [arXiv:1008.2024](#).
- [7] T. Kobayashi, Y. Nakai, and M. Sakai, *(Extra)Ordinary Gauge/Anomaly Mediation*, *JHEP* **1106** (2011) 039, [[arXiv:1103.4912](#)].
- [8] N. Okada, *Positively deflected anomaly mediation*, *Phys.Rev.* **D65** (2002) 115009, [[hep-ph/0202219](#)].
- [9] I. Jack and D. Jones, *Fayet-Iliopoulos D terms and anomaly mediated supersymmetry breaking*, *Phys.Lett.* **B482** (2000) 167–173, [[hep-ph/0003081](#)].
- [10] N. Arkani-Hamed, D. E. Kaplan, H. Murayama, and Y. Nomura, *Viable ultraviolet-insensitive supersymmetry breaking*, *JHEP* **02** (2001) 041, [[hep-ph/0012103](#)].
- [11] D. E. Kaplan and G. D. Kribs, *Gaugino-assisted anomaly mediation*, *JHEP* **0009** (2000) 048, [[hep-ph/0009195](#)].

- [12] Z. Chacko and M. A. Luty, *Realistic anomaly mediation with bulk gauge fields*, *JHEP* **0205** (2002) 047, [[hep-ph/0112172](#)].
- [13] R. Dermisek, H. Verlinde, and L.-T. Wang, *Hypercharged Anomaly Mediation*, *Phys.Rev.Lett.* **100** (2008) 131804, [[arXiv:0711.3211](#)].
- [14] J. de Blas, P. Langacker, G. Paz, and L.-T. Wang, *Combining Anomaly and Z-prime Mediation of Supersymmetry Breaking*, *JHEP* **1001** (2010) 037, [[arXiv:0911.1996](#)].
- [15] Z. Chacko, M. A. Luty, I. Maksymyk, and E. Ponton, *Realistic anomaly mediated supersymmetry breaking*, *JHEP* **0004** (2000) 001, [[hep-ph/9905390](#)].
- [16] R. N. Mohapatra, N. Setzer, and S. Spinner, *Minimal Seesaw as an Ultraviolet Insensitive Cure for the Problems of Anomaly Mediation*, *Phys. Rev.* **D77** (2008) 053013, [[arXiv:0707.0020](#)].
- [17] K. Choi, A. Falkowski, H. P. Nilles, and M. Olechowski, *Soft supersymmetry breaking in KKLT flux compactification*, *Nucl.Phys.* **B718** (2005) 113–133, [[hep-th/0503216](#)].
- [18] M. Endo, M. Yamaguchi, and K. Yoshioka, *A Bottom-up approach to moduli dynamics in heavy gravitino scenario: Superpotential, soft terms and sparticle mass spectrum*, *Phys.Rev.* **D72** (2005) 015004, [[hep-ph/0504036](#)].
- [19] B. S. Acharya, K. Bobkov, G. L. Kane, P. Kumar, and J. Shao, *Explaining the Electroweak Scale and Stabilizing Moduli in M Theory*, *Phys.Rev.* **D76** (2007) 126010, [[hep-th/0701034](#)].
- [20] M. A. Luty and R. Sundrum, *Radius stabilization and anomaly-mediated supersymmetry breaking*, *Phys. Rev.* **D62** (2000) 035008, [[hep-th/9910202](#)].
- [21] S. Kachru, L. McAllister, and R. Sundrum, *Sequestering in String Theory*, *JHEP* **0710** (2007) 013, [[hep-th/0703105](#)]. * Temporary entry *.
- [22] M. Luty and R. Sundrum, *Anomaly mediated supersymmetry breaking in four-dimensions, naturally*, *Phys.Rev.* **D67** (2003) 045007, [[hep-th/0111231](#)].
- [23] M. Schmaltz and R. Sundrum, *Conformal Sequestering Simplified*, *JHEP* **0611** (2006) 011, [[hep-th/0608051](#)].
- [24] B. Holdom, *Two $U(1)$'s and Epsilon Charge Shifts*, *Phys. Lett.* **B166** (1986) 196.
- [25] G. F. Giudice and A. Masiero, *A Natural Solution to the mu Problem in Supergravity Theories*, *Phys. Lett.* **B206** (1988) 480–484.
- [26] T. Gherghetta, G. F. Giudice, and J. D. Wells, *Phenomenological consequences of supersymmetry with anomaly induced masses*, *Nucl.Phys.* **B559** (1999) 27–47, [[hep-ph/9904378](#)].
- [27] D. Kaplan, G. D. Kribs, and M. Schmaltz, *Supersymmetry breaking through transparent extra dimensions*, *Phys.Rev.* **D62** (2000) 035010, [[hep-ph/9911293](#)].

- [28] Z. Chacko, M. A. Luty, A. E. Nelson, and E. Ponton, *Gaugino mediated supersymmetry breaking*, *JHEP* **0001** (2000) 003, [[hep-ph/9911323](#)].
- [29] P. Fayet and J. Iliopoulos, *Spontaneously Broken Supergauge Symmetries and Goldstone Spinors*, *Phys.Lett.* **B51** (1974) 461–464.
- [30] A. Djouadi, J.-L. Kneur, and G. Moultaka, *SuSpect: A Fortran code for the supersymmetric and Higgs particle spectrum in the MSSM*, *Comput.Phys.Commun.* **176** (2007) 426–455, [[hep-ph/0211331](#)].
- [31] **ALEPH** Collaboration, A. Heister *et. al.*, *Search for charginos nearly mass degenerate with the lightest neutralino in $e^+ e^-$ collisions at center-of-mass energies up to 209-GeV*, *Phys.Lett.* **B533** (2002) 223–236, [[hep-ex/0203020](#)].
- [32] **OPAL** Collaboration, G. Abbiendi *et. al.*, *Search for chargino and neutralino production at $s^{**}(1/2) = 192\text{-GeV}$ to 209 GeV at LEP*, *Eur.Phys.J.* **C35** (2004) 1–20, [[hep-ex/0401026](#)].
- [33] P. Batra, A. Delgado, D. E. Kaplan, and T. M. Tait, *The Higgs mass bound in gauge extensions of the minimal supersymmetric standard model*, *JHEP* **0402** (2004) 043, [[hep-ph/0309149](#)].
- [34] V. Barger, P. Langacker, H.-S. Lee, and G. Shaughnessy, *Higgs Sector in Extensions of the MSSM*, *Phys.Rev.* **D73** (2006) 115010, [[hep-ph/0603247](#)].
- [35] S. P. Martin, *Extra vector-like matter and the lightest Higgs scalar boson mass in low-energy supersymmetry*, *Phys.Rev.* **D81** (2010) 035004, [[arXiv:0910.2732](#)].
- [36] I. Jack, D. Jones, and S. Parsons, *The Fayet-Iliopoulos D term and its renormalization in softly broken supersymmetric theories*, *Phys.Rev.* **D62** (2000) 125022, [[hep-ph/0007291](#)].
- [37] R. Rattazzi, A. Strumia, and J. D. Wells, *Phenomenology of deflected anomaly mediation*, *Nucl.Phys.* **B576** (2000) 3–28, [[hep-ph/9912390](#)].
- [38] H. Baer, J. Mizukoshi, and X. Tata, *Reach of the CERN LHC for the minimal anomaly mediated SUSY breaking model*, *Phys.Lett.* **B488** (2000) 367–372, [[hep-ph/0007073](#)].
- [39] A. Barr, C. Lester, M. A. Parker, B. Allanach, and P. Richardson, *Discovering anomaly mediated supersymmetry at the LHC*, *JHEP* **0303** (2003) 045, [[hep-ph/0208214](#)].
- [40] H. Baer, R. Dermisek, S. Rajagopalan, and H. Summy, *Neutralino, axion and axino cold dark matter in minimal, hypercharged and gaugino AMSB*, *JCAP* **1007** (2010) 014, [[arXiv:1004.3297](#)].
- [41] J. F. Gunion and S. Mrenna, *Probing models with near degeneracy of the chargino and LSP at a linear $e^+ e^-$ collider*, *Phys.Rev.* **D64** (2001) 075002, [[hep-ph/0103167](#)].

- [42] M. Ibe, T. Moroi, and T. Yanagida, *Possible Signals of Wino LSP at the Large Hadron Collider*, *Phys.Lett.* **B644** (2007) 355–360, [[hep-ph/0610277](#)].
- [43] S. D. Thomas and J. D. Wells, *Phenomenology of Massive Vectorlike Doublet Leptons*, *Phys.Rev.Lett.* **81** (1998) 34–37, [[hep-ph/9804359](#)].
- [44] M. R. Buckley, L. Randall, and B. Shuve, *LHC Searches for Non-Chiral Weakly Charged Multiplets*, [arXiv:0909.4549](#).
- [45] D. M. Pierce, J. A. Bagger, K. T. Matchev, and R.-j. Zhang, *Precision corrections in the minimal supersymmetric standard model*, *Nucl.Phys.* **B491** (1997) 3–67, [[hep-ph/9606211](#)].
- [46] C. Chen, M. Drees, and J. Gunion, *Searching for invisible and almost invisible particles at e^+e^- colliders*, *Phys.Rev.Lett.* **76** (1996) 2002–2005, [[hep-ph/9512230](#)]. Addendum/Erratum in [hep-ph 9902309](#).
- [47] A. Djouadi, M. Muhlleitner, and M. Spira, *Decays of supersymmetric particles: The Program SUSY-HIT (SUSpect-SdecaY-Hdecay-InTerface)*, *Acta Phys.Polon.* **B38** (2007) 635–644, [[hep-ph/0609292](#)].
- [48] T. Sjostrand, S. Mrenna, and P. Z. Skands, *PYTHIA 6.4 Physics and Manual*, *JHEP* **0605** (2006) 026, [[hep-ph/0603175](#)].
- [49] P. Meade and M. Reece, *BRIDGE: Branching ratio inquiry / decay generated events*, [hep-ph/0703031](#).
- [50] J. Alwall, P. Demin, S. de Visscher, R. Frederix, M. Herquet, *et. al.*, *MadGraph/MadEvent v4: The New Web Generation*, *JHEP* **0709** (2007) 028, [[arXiv:0706.2334](#)].
- [51] **ATLAS** Collaboration, ATLAS-CONF-2011-086, “SUSY Search with jets and E_{miss}”.
- [52] **CMS** Collaboration, CMS-PAS-SUS-11-003, “Search for supersymmetry in all-hadronic events with alphaT”.
- [53] **CMS** Collaboration, CMS-PAS-SUS-11-004, “Search for supersymmetry in all-hadronic events with missing energy”.
- [54] **CMS** Collaboration, CMS-PAS-SUS-11-005, “Search for supersymmetry in all-hadronic events with MT2”.
- [55] **ATLAS** Collaboration, ATLAS-CONF-2011-098, “SUSY Search with bjets and E_{miss}”.
- [56] **D0** Collaboration, V. M. Abazov *et. al.*, *Search for scalar bottom quarks and third-generation leptoquarks in $p\bar{p}$ collisions at $\sqrt{s} = 1.96$ TeV*, *Phys.Lett.* **B693** (2010) 95–101, [[arXiv:1005.2222](#)].

- [57] **CDF** Collaboration, T. Aaltonen *et. al.*, *Search for the Production of Scalar Bottom Quarks in $p\bar{p}$ collisions at $\sqrt{s} = 1.96$ TeV*, *Phys.Rev.Lett.* **105** (2010) 081802, [[arXiv:1005.3600](#)].
- [58] N. Arkani-Hamed, A. Delgado, and G. Giudice, *The Well-tempered neutralino*, *Nucl.Phys.* **B741** (2006) 108–130, [[hep-ph/0601041](#)].
- [59] T. Moroi and L. Randall, *Wino cold dark matter from anomaly mediated SUSY breaking*, *Nucl.Phys.* **B570** (2000) 455–472, [[hep-ph/9906527](#)].
- [60] B. S. Acharya, G. Kane, S. Watson, and P. Kumar, *A Non-thermal WIMP Miracle*, *Phys.Rev.* **D80** (2009) 083529, [[arXiv:0908.2430](#)].
- [61] P. Grajek, G. Kane, D. Phalen, A. Pierce, and S. Watson, *Is the PAMELA Positron Excess Winos?*, *Phys.Rev.* **D79** (2009) 043506, [[arXiv:0812.4555](#)].
- [62] G. Kane, R. Lu, and S. Watson, *PAMELA Satellite Data as a Signal of Non-Thermal Wino LSP Dark Matter*, *Phys.Lett.* **B681** (2009) 151–160, [[arXiv:0906.4765](#)]. * Brief entry *.
- [63] **PAMELA** Collaboration, O. Adriani *et. al.*, *An anomalous positron abundance in cosmic rays with energies 1.5-100 GeV*, *Nature* **458** (2009) 607–609, [[arXiv:0810.4995](#)].
- [64] **PAMELA** Collaboration, O. Adriani *et. al.*, *PAMELA results on the cosmic-ray antiproton flux from 60 MeV to 180 GeV in kinetic energy*, *Phys.Rev.Lett.* **105** (2010) 121101, [[arXiv:1007.0821](#)].
- [65] A. Abdo, M. Ackermann, M. Ajello, W. Atwood, L. Baldini, *et. al.*, *Fermi LAT Search for Photon Lines from 30 to 200 GeV and Dark Matter Implications*, *Phys.Rev.Lett.* **104** (2010) 091302, [[arXiv:1001.4836](#)].
- [66] A. Abdo, M. Ackermann, M. Ajello, W. Atwood, L. Baldini, *et. al.*, *Observations of Milky Way Dwarf Spheroidal galaxies with the Fermi-LAT detector and constraints on Dark Matter models*, *Astrophys.J.* **712** (2010) 147–158, [[arXiv:1001.4531](#)]. * Temporary entry *.
- [67] T. R. Slatyer, N. Padmanabhan, and D. P. Finkbeiner, *CMB Constraints on WIMP Annihilation: Energy Absorption During the Recombination Epoch*, *Phys.Rev.* **D80** (2009) 043526, [[arXiv:0906.1197](#)].
- [68] **XENON100** Collaboration, E. Aprile *et. al.*, *Dark Matter Results from 100 Live Days of XENON100 Data*, *Phys.Rev.Lett.* (2011) [[arXiv:1104.2549](#)].
- [69] G. F. Giudice and R. Rattazzi, *Extracting Supersymmetry-Breaking Effects from Wave-Function Renormalization*, *Nucl. Phys.* **B511** (1998) 25–44, [[hep-ph/9706540](#)].
- [70] N. Arkani-Hamed, G. F. Giudice, M. A. Luty, and R. Rattazzi, *Supersymmetry-breaking loops from analytic continuation into superspace*, *Phys. Rev.* **D58** (1998) 115005, [[hep-ph/9803290](#)].

- [71] D. E. Morrissey, D. Poland, and K. M. Zurek, *Abelian Hidden Sectors at a GeV*, *JHEP* **07** (2009) 050, [[arXiv:0904.2567](#)].
- [72] S. P. Martin, *A Supersymmetry primer*, [hep-ph/9709356](#).